Lawrence Berkeley National Laboratory
Recent Work

Title
WAVELENGTH MODULATED SPECTRUM and ELECTRONIC PROPERTIES OF HfS?

Permalink
https://escholarship.org/uc/item/4r08r3vr

Author
Fong, C.Y.

Publication Date
1976

eScholarship.org Powered by the California Digital Library
University of California

Submitted to the Physical Review

LBL-4583
Preprint

WAVELENGTH MODULATED SPECTRUM AND ELECTRONIC PROPERTIES OF HfS_2

C. Y. Fong, J. Camassel, S. Kohn, and Y. R. Shen

RECEIVED
LAWRENCE
BERKELEY LABORATORY

MAR 4 1976

LIBRARY AND
DOCUMENTS SECTION

January 1976

Prepared for the U. S. Energy Research and
Development Administration under Contract W-7405-ENG-48

For Reference

Not to be taken from this room

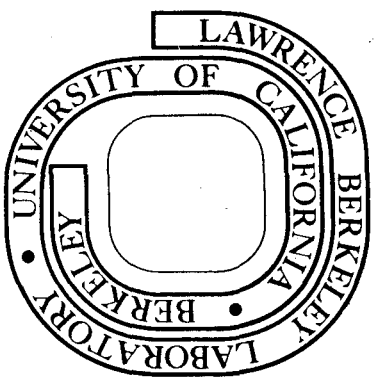

LBL-4583

DISCLAIMER

This document was prepared as an account of work sponsored by the United States Government. While this document is believed to contain correct information, neither the United States Government nor any agency thereof, nor the Regents of the University of California, nor any of their employees, makes any warranty, express or implied, or assumes any legal responsibility for the accuracy, completeness, or usefulness of any information, apparatus, product, or process disclosed, or represents that its use would not infringe privately owned rights. Reference herein to any specific commercial product, process, or service by its trade name, trademark, manufacturer, or otherwise, does not necessarily constitute or imply its endorsement, recommendation, or favoring by the United States Government or any agency thereof, or the Regents of the University of California. The views and opinions of authors expressed herein do not necessarily state or reflect those of the United States Government or any agency thereof or the Regents of the University of California.

0 0 0 0 4 4 0 8 0 3 1

Submitted to The Physical Review

LBL-4583

UNIVERSITY OF CALIFORNIA

Lawrence Berkeley Laboratory
Berkeley, California

AEC Contract No. W-7405-eng-48

WAVELENGTH MODULATED SPECTRUM AND ELECTRONIC PROPERTIES OF HfS_2

C. Y. Fong[§], J. Camassel[†], S. Kohn, and Y. R. Shen[*]

JANUARY 1976

[§]On sabbatical leave at Bell Laboratories, Murray Hill, New Jersey 07974.
Supported in part by the U.S. Air Force Office of Scientific Research (AFSC) under Grant No. AFOSR-72-2453.

[†]Present address: Laboratoire Electronique 2, C.E.E.S. - Faculte de Sciences, 34060 - Montpellier, Cedex - France.

[*]Supported by ERDA.

0 0 0 0 4 4 0 8 0 3 2

LBL-4583

Wavelength Modulated Spectrum and Electronic Properties of HfS_2

C. Y. Fong[§]
Department of Physics
University of California, Davis, California 95616

and

J. Camassel[†], S. Kohn and Y. R. Shen[*]
Department of Physics, University of California, and
Materials and Molecular Research Division,
Lawrence Berkeley Laboratory, Berkeley, California 94720

ABSTRACT

We have measured the reflectivity and the wavelength modulated reflectivity of HfS_2 at room temperature and 5°K. The reflectivity spectrum is compared with that obtained from a band structure calculated by the empirical pseudopotential method. Structures in the spectrum are identified. The volume effect of the optical transitions is shown to be important in this semiconducting layer crystal.

[§]On sabbatical leave at Bell Laboratories, Murray Hill, New Jersey 07974.
Supported in part by the U. S. Air Force Office of Scientific Research (AFSC) under Grant No. AFOSR-72-2453.

[†]Present address: Laboratoire Electronique 2, C.E.E.S. - Faculte de Sciencies, 34060 - Montpellier, Cedex - France.

[*]Supported by ERDA.

I. INTRODUCTION

Among the transition metal dichalcogenides, the group IVB compounds crystallize in the CdI_2 configuration. A typical layer consists of a plane of metal atoms sandwiched between two planes of the chalcogenides. In contrast to the polytypes of the group VB and VIB crystals,[1] there is only one stacking sequence. Within a layer, each metal atom is octahedrally surrounded by six chalcogens as shown in Fig. 1. The saturation of the p-orbitals in one formula unit suggests these compounds should be semiconductors. As expected, most of the Zr and Hf compounds (except the ditellurides) are semiconductors. Conflicting results about the fundamental properties of Ti-dichalcogenides have been found in the literature,[2] but we shall not pursue this subject here.

Experimentally, one of the most extensively studied group IVB semiconducting dichalcogneides is HfS_2 because good quality crystal can easily be obtained. Absorption measurements[4] support an indirect energy gap of value 1.96 eV at room temperature and a temperature coefficient of -4.3×10^{-4} eV/°K in the range of 77-500°K. An independent electrical determination[5] gives a slightly higher value of 2.1 eV. At liquid helium temperature, transmission measurements performed on thin adhesive cleaved samples[6] have been able to resolve some fine structures in the range 2.5-3.5 eV.

Theoretical band structure calculations on HfS_2 have been performed by Murray, et al (MBY)[1] and by Mattheiss.[3] MBY used a semi-empirical tight-binding scheme with three empirical parameters. These parameters

0 0 0 0 4 4 0 8 0 3 3

were used to weigh the calculated overlapping integrals and were determined by assigning a priority: (i) an indirect gap $\Gamma_2^- \rightarrow L_1^+$ at 2.08 eV; (ii) $L_1^- \rightarrow L_1^+$ at 2.87 eV; and (iii) $\Gamma_3^- \rightarrow \Gamma_1^+$ at 3.4 eV. In an attempt to explain the data of the transmission measurements,[6] they calculated the joint density of states of ZrS_2 and extended it to HfS_2. On the other hand, the augmented plane-wave method (APW) has been applied by Mattheiss to calculate the band structure of HfS_2 at a few important $\vec{k}$-points in the Brillouin zone (BZ). The band structure along symmetry directions was then obtained by Slater-Koster's tight-binding interpolation scheme. The results suggest an indirect gap $\Gamma_2^- \rightarrow L_1^+$ at 2.77 eV. No serious comparison with the experimental data has been made in this case.

Even in this simple semiconducting transition metal layer compound, comparisons between the experimental and the theoretical results have been previously restricted to a semiquantitative basis because of lack of the dipole transition matrix elements[1,3] and the two-dimensional nature of the theoretical approach.[1] For better understantding of transition-metal dichalogenides a more realistic comparison between theory and experiment is necessary. In this paper, we report our measurements on the reflectivity and wavelength modulated reflectivity of HfS_2 at room temperature and liquid helim temperature in the range of 2-6 eV. We also present a band structure of HfS_2 obtained from the empirical pseudopotential method (EPM). The experimental reflectivity spectrum is then compared with the theoretical reflectivity spectrum deduced from the band structure calculation. We believe that this is the first realistic

comparison ever made on such layer compounds.

We have arranged this paper in the following way: Sections II and III briefly describe the experimental arrangement and theoretical method respectively. Section IV is a discussion and comparison of the present measured and calculated results as well as a comparison with various earlier experimental and theoretical work on the crystal.

II. EXPERIMENT

The HfS_2 crystal we used had a broad face of 1 cm x 0.5 cm and a thickness of about 10 μ. The latter was deduced from the interference fringes shown in Fig. 2 around 2.2 eV. The C axis of the crystal was perpendicular to the platelet. Because of the small sample thickness, our optical measurements were restricted to the configuration $\vec{E} \perp \hat{C}$. The sample was mounted on a sample holder free of strain and an "as grown" natural face of the platelet was used for the optical measurements.

The experimental apparatus for simultaneous measurements of the reflectivity and the logarithmic derivative of the reflectivity has been described elsewhere.[7] In order to facilitate comparison with theory, the data were digitized and converted from wavelength to energy scale on a computer. The results are presented in Fig. 2.

III. THEORY

The empirical pseudopotential method has been discussed in detail in the literatures.[8] In essence, a nonlocal pseudopotential with

0 0 0 0 4 4 0 8 0 3 4

$\ell = 2$ centered at the Hf-atom in the unit cell was used to account for the strong potential experienced by the partially filled d-electrons. The potentials of the s- and p-electrons and some of the hybridization effects in the crystal are expressed in terms of the form factors of the local pseudopotentials. The starting form factors of the S-atom was scaled from SnS_2.[9] As the form factors of Hf have never been reported in the literature, they were initially approximated by the pseudopotential of the Nb-atom[10] with proper scaling. These atomic form factors were cutt off at $|\vec{G}|^2_{max} = 15\ (\sqrt{2}\pi/a)^2$, where $\vec{G}$ is a reciprocal lattice vector and a is the lattice constant in the X-Y plane. This results in a total of 17 nonvanishing form factors for each atomic species. To secure proper convergence of the band energies with respect to the number of plane waves, we used control energies[8] $E_1 = 19.5$ and $E_2 = 37.5$ in units of $(\sqrt{2}\pi/a)^2$. Equivalently, there are about 185 plane waves with energies less than E_1 and about 300 plane waves used in the Lowin-Brust perturbation scheme.[11] The convergence of the calculated energies at Γ, K, A and H is within 0.1 eV, whereas at M and L it is only of the order of 0.1 eV. Spin-orbit interaction is neglected in the present calculation.

To calculate the reflectivity from the band structure we calculate first the imaginary part of the dielectric function, $\varepsilon_2(\omega)$, by the linear interpolation scheme.[12] There are 60 $\vec{k}$-points in the (1/12)th of the BZ used to set up the mesh. Since we anticipate a comparison of $R(\omega)$ with $\vec{E} \perp \hat{C}$, only the perpendicular components of the dipole transition

matrix elements of six valence bands[3-8] to five conduction bands[9-13] were considered at the mesh points. An equivalent of 2.5×10^4 points in the BZ were sampled. Then, we used the Kramer-Kronig relation to calculate the real part of the dielectric function, $\varepsilon_1(\omega)$, and the reflectivity $R(\omega)$.

IV. RESULTS AND COMPARISONS

In Fig. 2 the reflectivity, $R(\omega)$, and its logarithmic derivative were plotted as functions of photon energy, $\hbar\omega$. In general, the reflectivity shows prominent structures for $\hbar\omega \leq 3.5$ eV, a strong drop-off above 4.0 eV and a fairly constant "plateau" observed up to 6 eV. The minimum of the reflectivity at 4.23 eV is only about 2%. The magnitude of the reflectivity of the "plateau" is sensitive to the position of the focused beam on the sample surface. As usual, the derivative spectrum displays many fine structures. We shall compare later the details of other experimental and theoretical results.

The calculated band structure along several symmetry directions is shown in Fig. 3. We have used Slater's notations of the irreducible representations for the D_{3d} group. The labelings at L are different from those used in Ref. 3, but are equivalent with $1 \leftrightarrow 1^+$. $2 \leftrightarrow 1^-$, $3 \leftrightarrow 2^-$ and $4 \leftrightarrow 2^+$. From now on, we shall use the notations without the "+" and "-" signs at L. In Fig. 4, we compare our experimental and calculated reflectivity spectra.

The calculated indirect fundamental gap is the transition of $\Gamma_2^- \rightarrow M_1^+$ at 1.8 eV which agrees to $\sim$ 0.2 eV with the experimental value.

0 0 0 0 4 4 0 8 0 3 5

Although our idenficiation differs from the one ($\Gamma_2^- \rightarrow L_1$) given by Refs. 1 and 3, it may not be incompatible. As shown in Fig. 3, the energy of the lowest conduction band (the 9th band) at $L(L_1)$ is 0.1 eV about M_1^+ while the convergence of energy at both L and M points, as we discussed in previous section, is only of the order of 0.1 eV. It is quite possible that with finer matrices, the relative ordering of L_1 and M_1^+ is reversed. As a comparison, we note that the indirect gap calculated by MBY is 2.7 eV (as deduced from the band structure of HfS_2 in Ref. 1). Similar discrepancy appears in the other identified structures.

The first prominent structure in our experimental reflectivity spectrum is a 2.83 eV. Compared to the value reported by Greenaway and Nitche[4] (2.9 eV) and the one given by Beal et al[6] (2.88 eV), our peak is about 60 meV lower. This difference may be due (a) to the increased accuracy achieved in the modulation spectroscopy, and (b) to the shift of peak energies between absorption and reflectivity spectra[13,14]. The theoretical spectrum in this range shows a weak shoulder at 2.7 eV and a peak at 2.9 eV. We assign the peak to the observed structure at 2.83 eV. Both theoretical structures come from regions near Δ (line $\Gamma \rightarrow A$) from transitions of the upper most valence band to the lowest conduction band ($8 \rightarrow 9$ transitions) except that the 2.7 eV contour does not enclose the point A. We find no correlation of this structure with the point L in the BZ as suggested by MBY.[1] Their calculated energies of transitions $L_2 \rightarrow L_1$ and $L_3 \rightarrow L_1$ (assigned by MBY as the direct gap) are at 3.47 and 3.6 eV respectively. Hence, it will be impossible to account for the 2.83 eV experimental

structure in a spectrum deduced from their band structure. The result of the APW calculation[3] suffers the same shortcoming, since the calculated minimum direct gap at 3.43 eV is also at L. From our calculation, we suggest that the fundamental direct gap of HfS_2 is at $\Gamma(\Gamma_2^- \rightarrow \Gamma_3^+)$ with a gap energy of 2.4 eV and rather weak dipole transition matrix elements, and the contribution to the 2.83 eV structure is due to the volume effect.[8]

The two next structures around 2.94 and 2.99 eV in the derivative reflectivity spectrum agree with the ones at 3.03 and 3.07 eV in the transmission data[6]. The splitting in our case is 50 meV, and agrees with the value (~65 meV) calculated by MBY for the spin-orbit splitting of the $\Gamma_3^{-(6,7)}$ band. However, the interband energy of $\Gamma_3^- \rightarrow \Gamma_1^+$ given by MBY is 4.08 eV which is about 1 eV higher than the measured value of the structure. Beal et al[6] identified the 3.07 eV shoulder as the transitions associated with $M_1^- \rightarrow M_1^+$, i.e., $8 \rightarrow 9$ at M. Our theoretical result shows a shoulder at 3.1 eV. It is not resolved into two structures since the resolution of the calculation is only 0.1 eV. The contributions to this structure are from $8 \rightarrow 9$ transitions near the L point and $7, 8 \rightarrow 11$ transitions around the A point. Both regions have strong dipole matrix elements. Since part of the contributions associated with the degenerate valence bands at the point A ($A_3^- \rightarrow A_1^+$), it is possible that the 50 meV splitting is due to spin-orbit splitting of these degenerate bands.

The 3.2 eV structure in Refs. 4 and 6 is seen in our experimental spectrum (Fig. 2) as a shoulder at 3.17 eV with no splitting resolved. The transition possibly responsible for the structure is $L_2 \rightarrow L_1 (7 \rightarrow 9)$

0 0 0 0 4 4 0 8 0 3 6

but its contribution is not visible in our calculated spectrum as it is masked by the strong peak at 3.3 eV.

Both our experimental and theoretical spectra show a strong peak at 3.3 eV, which presumably corresponds to the 3.23 eV peak in the absorption spectrum. This peak was identified in Ref. 1 as due to $\Gamma_3^- \rightarrow \Gamma_1^+$ transitions. Their calculated energy os this peak was however, at 4.08 eV. We find from our calculation that the peak comes from 8 → 9 transitions in an extended region very near the ΓALM plane in the BZ. a nearby critical point with M_1 symmetry is found along R $[(\frac{1}{3},0;\ \frac{1}{2})\ \frac{\sqrt{2}\pi}{a}]$ at 3.25 eV. The strong dipole transition matrix elements near the plane enhance the intensity of the peak.

In the higher energy region, both spectra in Fig. 4 show a structure at 3.5 eV which can be attributed to the $M_1^- \rightarrow M_1^+$ (8 → 9) transitions. The theoretical spectrum has a structure at 3.9 eV which differes from the experimental structure at 3.8 eV by 0.1 eV and is due to the volume effect in two extended regions: (a) 8 → 9 transitions with cylindrical contour surface intersecting the midpoints of the S and T lines and the zone boundaries near L and M since the dipole matrix elements of 8 → 9 transitions decrease sharply as the $\bar{k}$-points move away from the ΓALM plane, the strength of the structure is weaker than the 3.3 eV peak; (b) 7 → 9 transitions with contour surface almost parallel to the AΓLM plane. The dipole matrix elements associated with these transitions are weak. The peak at 4.4 eV is mainly due to the 7 → 9 transitions with contours similar to the one given in (b) except it is farther away from AΓLM planes.

A fast drop in the reflectivity around 4.1 eV is exhibited in both spectra, although the one in the theoretrical spectrum appears to be less drastic. A similar dip has been observed in Refs. 4 and 6. Our calculation shows that this is due to exhaustion of oscillator strength of the $8 \rightarrow 9$ and $7 \rightarrow 9$ transitions. The experimental reflectivity starts arising gradually after 4.2 eV and reaches a weak maximum at 4.9 eV. This is in good agreement with the result of Greenaway and Nitche.[6] The corresponding structure in the theoretical specrum is 0.3 eV lower and the magnitude is about seven times higher. The main contribution to this peak comes from $7 \rightarrow 10$ transitio-s in the region near Δ but above the ΓMK plane. The discrepancy in the higher region has been found in most pseudopotential calculations of semiconductors[8]. We have summarized the above discussion in Table I.

Compared with other theoretical calculations, the band ordering near the gap shown in Fig. 3 agrees well with the APW results[3] but differs from the tight-binding calculation which shows Γ_1+ being the lowest conduction band. A detailed comparison of the band energies at Γ and L with respect to Γ_2- and the ordering of the bands near the gap is given in Table II. Our Γ_3+ (3rd and 4th bands) and Γ_1+ (5th band) are reversed with respect to the other two calculations. This can be an artifact due to imposition of smoothness for the pseudopotential form factors. The (3s)-bands of the S-atoms are about 15. eV below the top of the valence band. The accuracy of these bands may be tested in the future by the soft x-ray photoesmission (XPS) measurements. It is

0 0 0 0 4 4 0 8 0 3 7

interesting to compare the widths of the nonbonding d bands and the uppermost p bands obtained in different calculations as listed in Table I. We take the maximum separation of the energies between the 9th and 11th bands for the width of the d-states and that between the 7-th and 8-th bands of the width of the p-states. The bandwidths of the present calculation in both cases are wider than those of Ref. 1 and 3.

In conclusion, we have measured the reflectivity and the first-order derivative reflectivity spectra of HfS_2 at room temperature and at 5°K. The structures agree well with earlier experimental results and are in reasonable agreement with those derived from the band structure calculation using the empirical pseudopotential method. Structures below $\hbar\omega$ = 5.0 eV have been identified. Prominent peaks at $\hbar\omega \leq 3.5$ eV come from transitions from two uppermost valence bands (p-states) to the lowest nonbanding d states in a large region of the BZ. This is contrary to the earlier identifications[1] which associate strong peaks with only a few critical points in the BZ. Comparison of the present calculation tight-binding and APW calculations shows that: (1) The band ordering near the gap agrees with the APW results but differs from the tight-binding results; (2) the two uppermost p and the nonbonding d conduction bands are wider by a factor of 2 in empirical pseudopotential calculation than those in the other calculations.

ACKNOWLEDGEMENTS

We thank Dr. Levy and Dr. H. Berger from the Laboratoire de Physique Appliquee Ecole Polytechnique Federate de Lausanne for the growth and supply of the sample used in this experiment.

REFERENCES

1. R. B. Murray, R. A. Bromley and A. D. Yoffe, J. Phys. C 5, 746 (1972).

2. See for example, H. W. Myron and A. J. Freeman, Phys. Lett. 44A, 167 (1973).

3. L. F. Mattheiss, Phys. Rev. B8, 3719 (1973).

4. D. L. Greenaway and R. Nitsche, J. Phys. Chem. Sol. 26, 1445 (1965).

5. L. E. Conroy and K. C. Park, Jung. Chem. 7, 459 (1968).

6. A. R. Beal, J. C. Knights and W. Y. Liang, J. Phys. C 5, 3531 (1972).

7. R. R. L. Zucca and Y. R. Shen, Appl. Optics 12, 1293 (1973); Y. R. Shen, Surf. Sciences 27, 522, (1973).

8. M. L. Cohen and V. Heine, Solid State Phys. 24, 37 (1970); C. Y. Fong and M. L. Cohen, Phys. Rev. Lett. 24, 306 (1970).

9. C. Y. Fond and M. L. Cohen, Phys. Rev. B5, 3095 (1972).

10. C. Y. Fong and M. L. Cohen, Phys. Rev. Lett. 32, 720 (1974).

11. D. Brust, Phys. Rev. 134A, 1337 (1964).

12. W. M. Saslow, T. K. Bergstresser, C. Y. Fong, M. L. Cohen and D. Brust, Solid State Comm. 5, 667 (1967).

13. M. Welkowsky and R. Baunstein, Phys. Rev. b5, 497 (1972).

14. S. E. Kohn, P. Y. Yu, Y. Petroff, Y. R. Shen, Y. Tsang, and M. L. Cohen, Phys. Rev. B8, 1477, (1973).

15. J. A. Wilson and A. D. Yoffe, Advances in Phys. 18, 193 (1969).

0 0 0 0 4 4 0 8 0 3 8

FIGURE CAPTIONS

Fig. 1 a. Hexogonal unit cell of HfS_2.

b. Octohedral continuation within one layer.

Fig. 2 The wavelength modulated reflectivity at 5°K and the reflectivity at 5°K (——) and at 300°K(- - -).

Fig. 3 The band structure of HfS_2.

Fig. 4 The experimental and theoretical spectra of HfS_2.

TABLE CAPTIONS

Table I Comparison of experimental and theoretical critical point energies and their assignments. All energies are in eV.

Table II Comparison of the band ordering and eigeuvalues at Γ and L in different band strucutre calculations. (All energies are in eV).

0 0 0 0 4 4 0 8 0 3 9

TABLE I

	THEORY				EXPERIMENT		
Authors / Feature	Wilson Yoffe	Present Work	Murray[1] Brumley Yoffe†	Mattheiss[3]	Greenaway[4] Nitsche	Beal[6] Knight Liang	Present Work
Indirect Gap	1.98	1.8 ($\Gamma_2^- \rightarrow M_1^+$)	(2.7) ($\Gamma_2^- \rightarrow L_1^+$)	2.77 ($\Gamma_2^- \rightarrow L_1^-$)	1.96		
Direct Gap		2.4 ($\Gamma_2^- \rightarrow \Gamma_3^+$)	3.47 ($L_3^- \rightarrow L_1^-$)	3.43 ($L_3^- \rightarrow L_1^-$)			
Optical Structure		2.9 {8 → 9 near Δ}	3.6 ($L_2^- \rightarrow L_1^-$)		2.9	2.88	2.83
		3.1 {$L_3^- \rightarrow L_1^+$, $A_3^- \rightarrow A_1^+$}				3.03, 3.07 ($M_1^- \rightarrow M_1^+$)	2.94 2.99
		3.16 ($L_2^- \rightarrow L_1^-$)			3.2	3.2	3.17
		3.3 {8 → 9 ($\frac{1}{3}, 0, \frac{1}{2}$) $\sqrt{2}\pi$ and a near ΓALM plane}	4.08 ($\Gamma_3^- \rightarrow \Gamma_1^+$)			3.23	3.3
		3.5 ($M_1^- \rightarrow M_1^+$)					3.5
		3.9 {8→9, 7→9 Volume effect}					3.8
		4.4 {7→ 9 Volume effect}					
		4.6 {7 → 10 Volume effect}			5.0		4.9
Width of the nonboundary d-bands	1.98	4.0 ($L_1^+ \rightarrow L_1^-$)	3.14 ($M_1^+ \rightarrow M_1^+$)	3.31 ($M_1^+ \rightarrow M_1^+$)			
Width of the uppermost p-band	0.87	3.1 ($H_1^- \rightarrow \Gamma_2^-$)	1.56 ($M_2^- \rightarrow \Gamma_2^-$)	1.54 ($M_2^- \rightarrow \Gamma_2^-$)			

† Values deduced from the band structure.

TABLE II

Feature	Ordering of levels at Γ, neglecting S.O. interaction.			Ordering of levels at L, neglecting S.O. interaction.		
	Present work	MBY	Mattheiss	Present work	MBY	Mattheiss
Minimum of the C.B.	Γ_1^+ (2.7eV) Γ_3^+ (2.4 eV)	Γ_3^+ (4.8eV) Γ_1^+ (3.7 eV)	Γ_1^+ (4.2eV) Γ_3^+ (3.9 eV)	L_1 (L_1^+) (1.9 eV)	L_1^+ (2.7 eV)	L_1^+ (2.7 eV)
Top V.B.	Γ_2^-	Γ_2^-	Γ_2^-	L_3 (L_2^-) (-1.15 eV)	L_2^- (-0.7 eV)	L_2^- (-0.7 eV)
Second V.B.	Γ_3^- (-0.1 eV)	Γ_3^- (-0.4 eV)	Γ_3^- (-0.2 eV)	L_2 (L_1^-) (-0.1 eV from L_3)	L_1^- (-0.14 eV from L_2^-)	L_1^- (-0.1 eV from L_2^-)

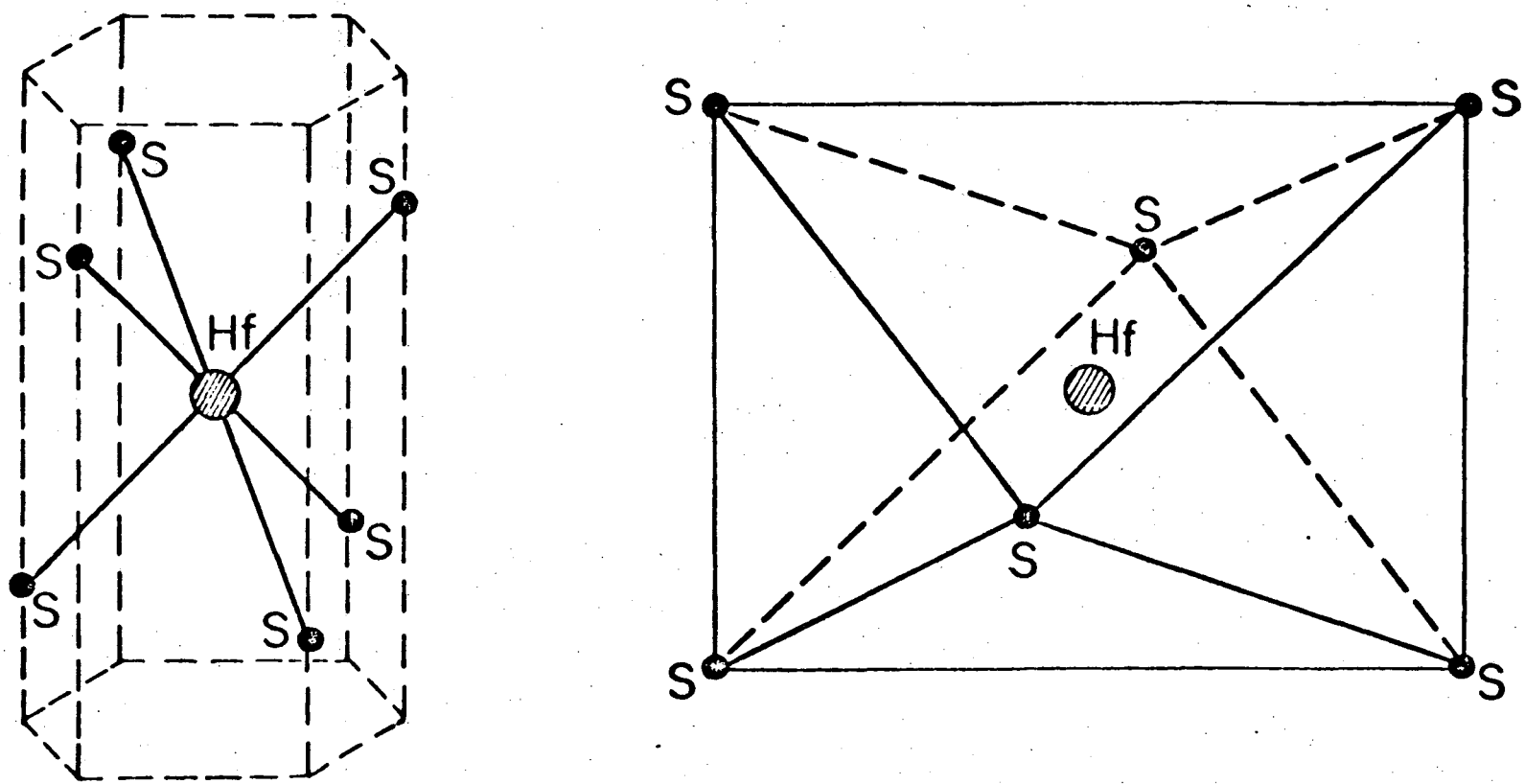

XBL 759-7161

Fig. 1

DISCLAIMER

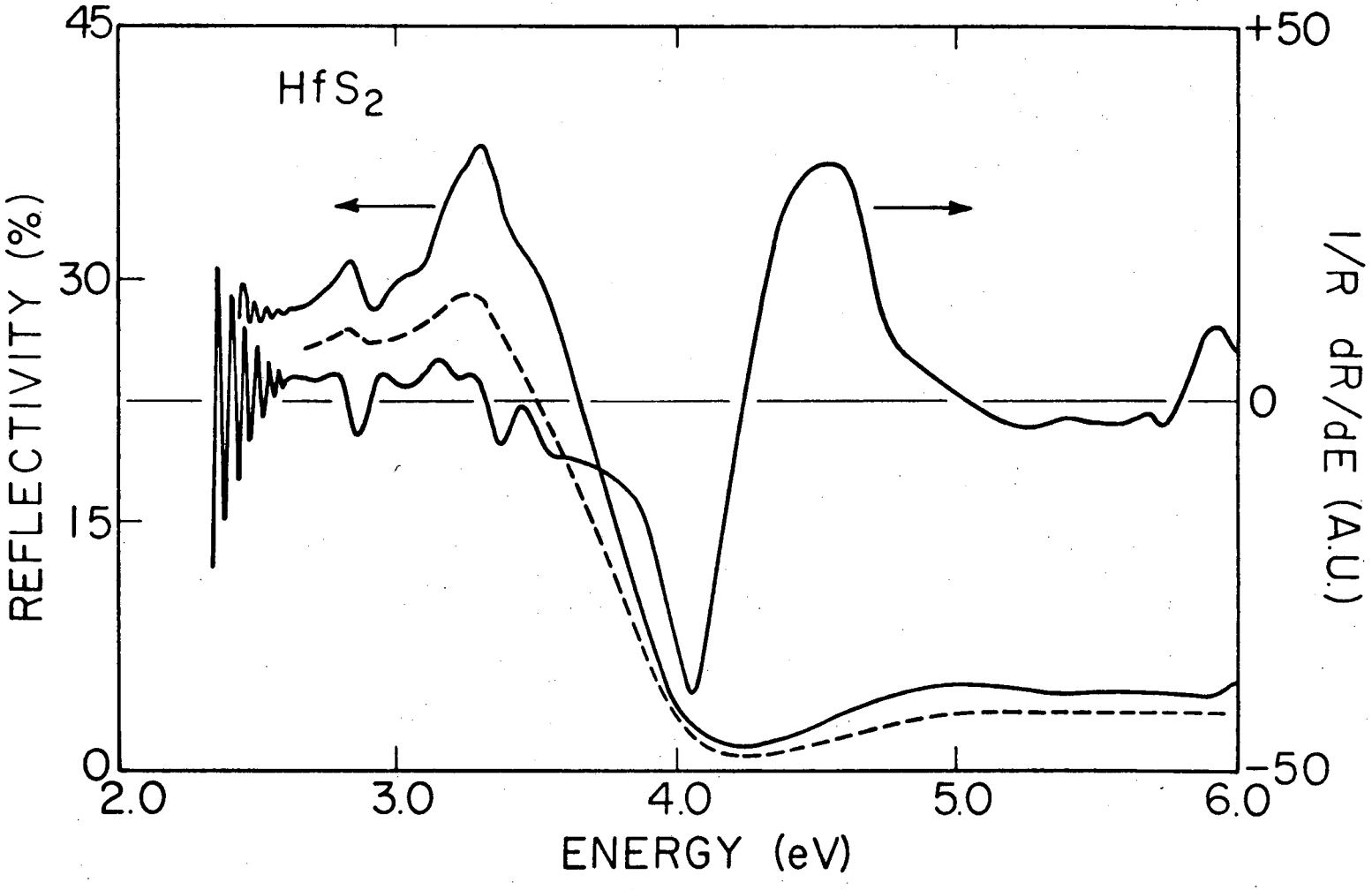

XBL 7511-7581

0 0 0 0 4 4 0 8 0 4 1

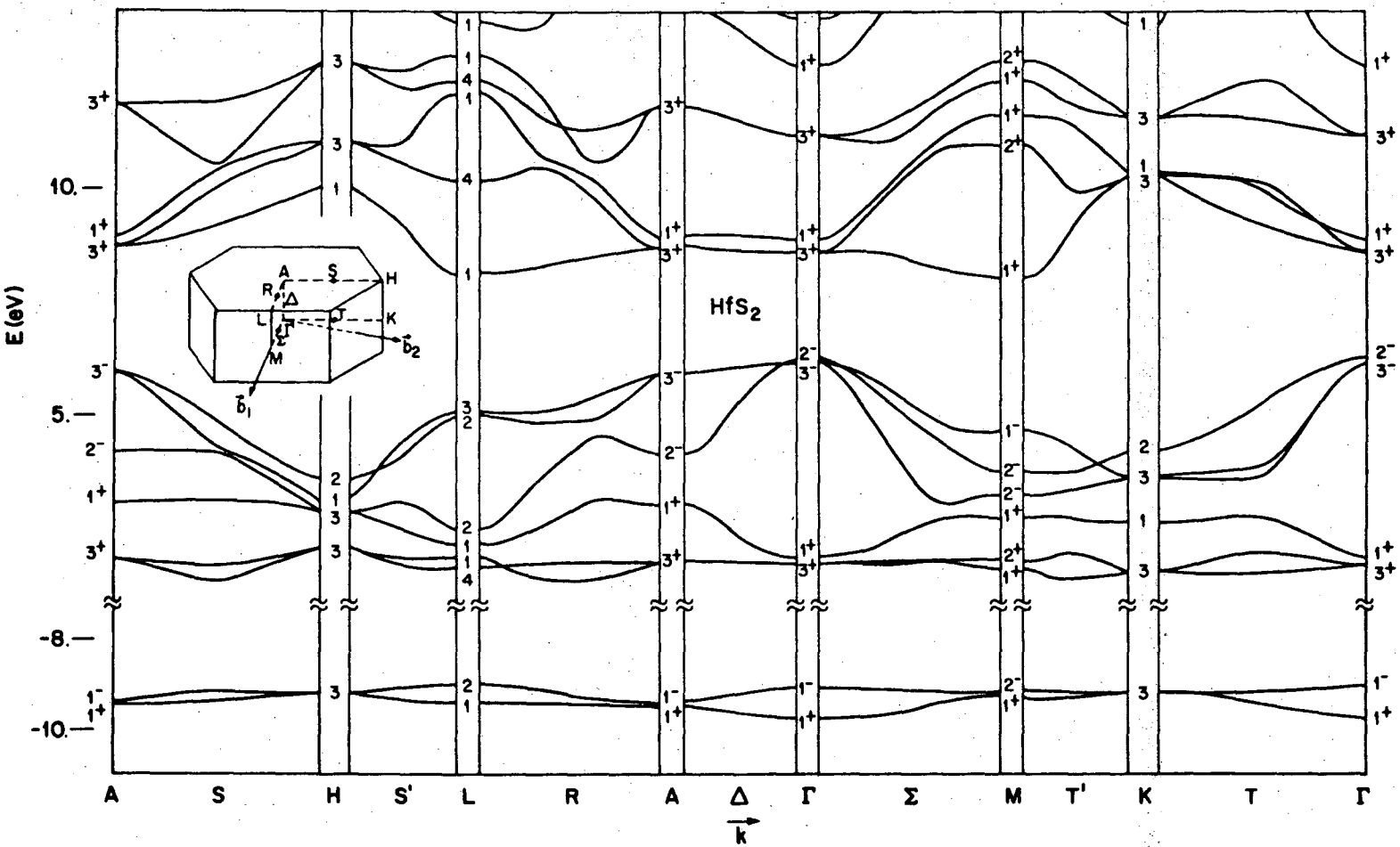

XBL 761-6178

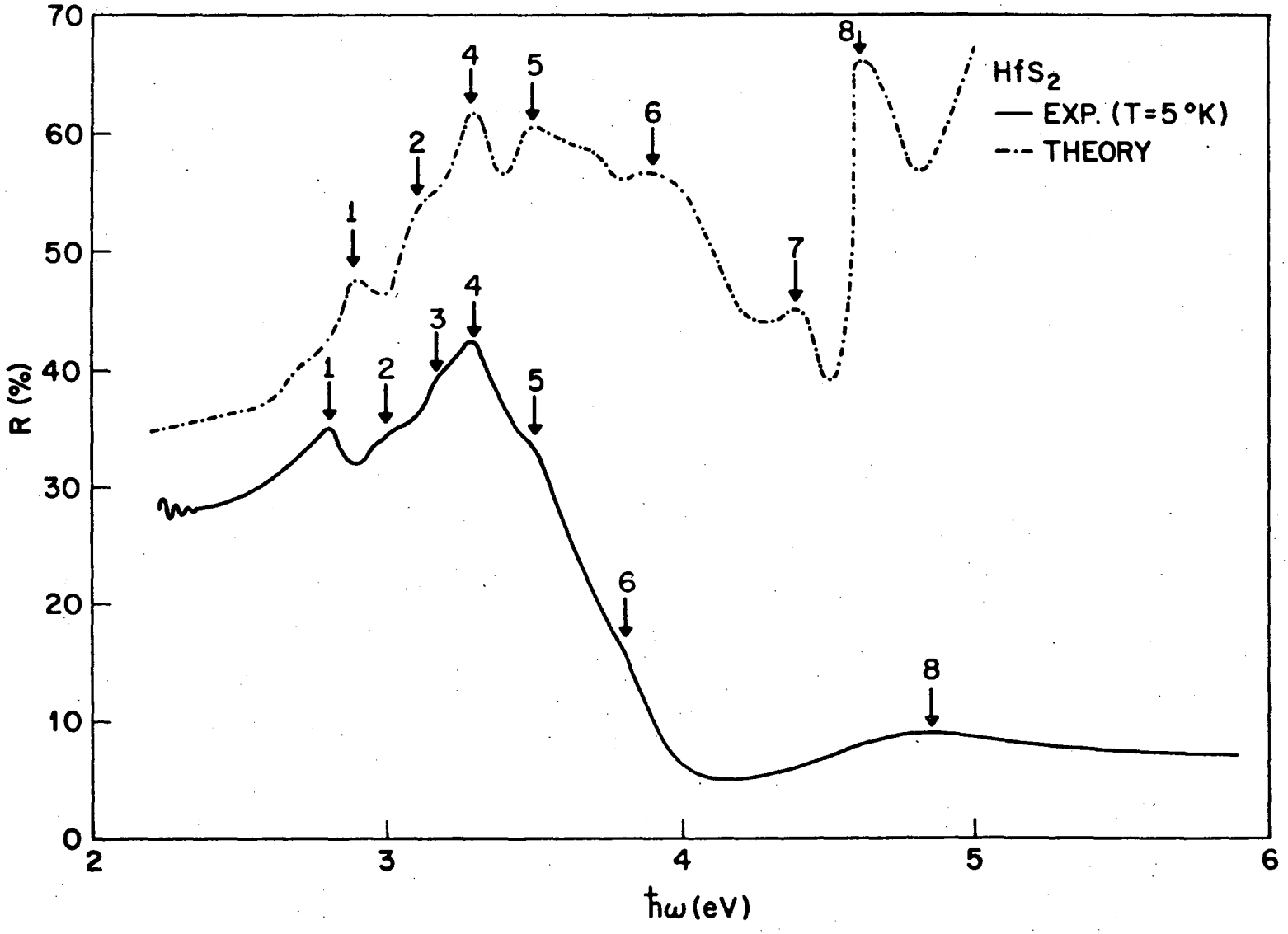
70
60
50
40
30
20
10
0
R (%)
2
3
4
5
6
ħω (eV)
HfS2
— EXP. (T=5°K)
-·- THEORY
1
2
3
4
5
6
7
8
1
2
4
5
6
8

XBL 761-6179

LEGAL NOTICE

This report was prepared as an account of work sponsored by the United States Government. Neither the United States nor the United States Energy Research and Development Administration, nor any of their employees, nor any of their contractors, subcontractors, or their employees, makes any warranty, express or implied, or assumes any legal liability or responsibility for the accuracy, completeness or usefulness of any information, apparatus, product or process disclosed, or represents that its use would not infringe privately owned rights.

TECHNICAL INFORMATION DIVISION
LAWRENCE BERKELEY LABORATORY
UNIVERSITY OF CALIFORNIA
BERKELEY, CALIFORNIA 94720